Influence of orientation on coadsorption dynamics: CO displacement from a $c(2\times2)$ precovered Ni(100) surface by free oriented NO

H. Müller, B. Dierks, G. H. Fecher,[a] N. Böwering, and U. Heinzmann
Universität Bielefeld, Fakultät für Physik, 33501 Bielefeld, Germany

(Received 7 February 1994; accepted 8 June 1994)

Collision experiments between two different molecules both oriented with their axis are presented: The kinetics of the CO desorption and NO sticking probability by oriented NO has been investigated using supersonic molecular beam and work function techniques. The work function measurements exhibit mainly molecular adsorption of NO on a CO precovered Ni(100) surface at $T=300$ K. The desorption and the sticking depend strongly on the initial orientation of the NO molecules in the gas phase. The sticking probability is higher for preferential N-end collisions and the sticking asymmetry is constant, whereas the desorption asymmetry changes its sign from initially negative to positive values, depending on the exposure time or NO coverage. We explain the asymmetries by two different mechanisms, namely direct and indirect molecular exchange. N-end collisions lead preferentially to NO sticking and NO induced CO desorption, whereas O-end collisions enhance the direct CO displacement.

I. INTRODUCTION

Directional factors can influence the outcome of reactive molecular processes substantially, since directionally dependent properties can affect the efficiency of product formation leading to orientational effects, the so-called steric effect. Such directional influences can be studied when one reactant is bound to a surface with a fixed orientation and the other is prepared with specific orientations in the gas phase using state selection by a hexapole technique and subsequent orientation in a homogeneous electrical field.[1,2] In recent years investigations of orientational effects aiming at a better understanding of directional molecule-surface processes and the corresponding interaction potentials have been carried out by directing supersonic beams with oriented molecules onto single crystal surfaces.

Direct inelastic scattering, trapping/desorption, and sticking were observed to depend on the initial orientation of the molecules before their collision with the surface. Steric effects of scattering and trapping/desorption of free oriented NO molecules from Pt(111) and Ag(111) were found at the FOM (Amsterdam, Netherlands).[3–11] The Bernstein group used the combined fields technique to study steric effects in the scattering of CH_3F and other symmetric top molecules from graphite(0001).[12–14] We have examined the orientation dependence of sticking and scattering of NO at Ni(100).[15–18] Furthermore, calculations corresponding to the Amsterdam results have been published.[19–21]

The adsorption of molecules on surfaces provides also a restricted directional range due to the particular orientation of the adsorbate. Therefore, oriented beam-surface coadsorption experiments offer the possibility to investigate processes involving *two* oriented reactants. We report on such studies using free NO molecules oriented in two diametrical configurations before the collision with a Ni(100) surface which is precovered with a monolayer of oriented CO molecules bound with the C end to the surface.

Exposing a metal substrate to CO and NO may give rise to catalytic reactions leading to products such as N_2 and CO_2. This behavior has already been investigated on platinum[22] or rhodium [23] and has been used successfully in automotive exhausts as a catalyst, for instance. In the case of CO–NO coadsorption on Ni(100), a different kind of process was observed.[24] At low temperatures, the NO bond prevails and no new reaction products are formed; rather, the NO induces desorption of the CO resulting in an exchange of the adsorbate layer. This exchange can be described as "displacement,"[24] since the CO leaving (desorbing from) the surface is observed. Catalytic reactions are not found for NO on Ni(100) because at temperatures above 200 K the NO starts to dissociate giving rise to tightly bound atomic nitrogen forming a resistant NiN surface.

The adsorption of both CO and NO on nickel surfaces has been investigated frequently. Ni(100) covered by a saturated layer of CO represents the initial adsorption system. The CO chemisorption occurs molecularly at on-top sites with a perpendicular direction of the axis and the carbon end closest to the surface. At room temperature a monolayer coverage with a $c(2\times2)$ superstructure is observed by low-energy electron diffraction (LEED).[25–27] The CO–Ni bond[28] results in a reduction of electronic charge in the bond between C and O and in the σ-like antibonding states of C–Ni. The charge is transferred into π states causing the C–O bond to weaken and a C–Ni bond to be formed. This is termed "σ donation and π back donation" process.[29,30] Ni(100) covered by a saturated layer of NO represents the final adsorption system, since NO efficiently displaces CO. NO chemisorption on Ni(100) proceeds molecularly at low temperatures: however, the adsorbate starts to dissociate at least partially above 200 K.[31,32] At high coverage, the NO molecules are adsorbed with the nitrogen atom pointing to the surface.[33] A tilt angle of the NO axis, which was observed at different coverages is still under dispute.[33–37] At 300 K, the partially

[a]Permanent address: Johann Gutenberg-Universität Mainz, Institut für Physik, 6500 Mainz, Germany.

 0021-9606/94/101(8)/7154/7/$6.00

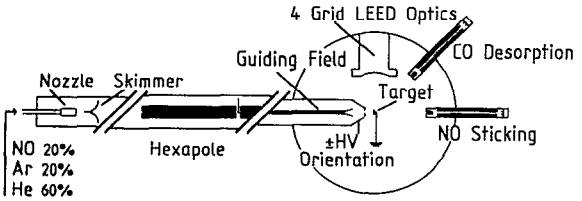

FIG. 1. Experimental setup of the supersonic beam, orientation arrangement and UHV chamber.

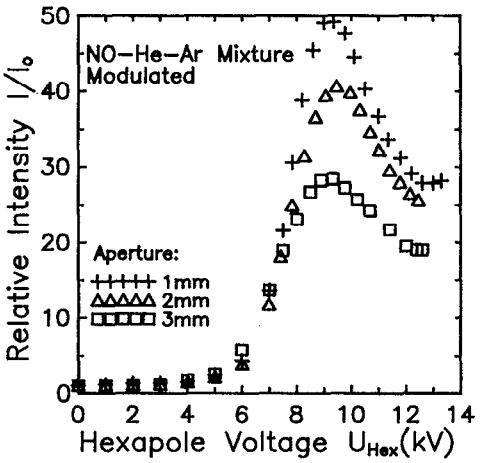

FIG. 2. Focusing spectra of the hexapole: relative intensity of the incident beam as a function of U_{hex} and aperture diameter normalized to the beam intensity at $U_{\text{hex}}=0$ kV.

dissociated molecules form a N, O.[34,37] NO $c(2\times2)$ superstructure as indicated by LEED.[32]

II. EXPERIMENT

The general idea of the experimental set up is given in Fig. 1. The left side displays the preparation of the supersonic NO beam, the right side shows the UHV chamber including the required detectors. The nozzle (diameter 80 μm) is operated in a continuous mode and with a gas mixture of NO (20%), Ar (20%), and He (60%) at a nozzle temperature of approximately 300 K and a stagnation pressure of 1300 mbar resulting in a translational energy of 125 meV. Behind the skimmer the NO molecules pass through the hexapole assembly, consisting of two hexapoles with six rods (total length 1700 mm) alternately held at voltages of $U_{\text{hex}}=\pm9.5$ kV. Taking advantage of the positive Stark effect, the divergent NO beam is then focussed onto the target,[15,16,38] which is located at a distance of 3.38 m from the nozzle. Depending on the field strength the hexapole selects different rotational states of the beam. To achieve a high degree of orientation, the NO ground state is chosen. In order to avoid rapid field variations and to keep the NO molecules in this $^2\Pi_{1/2}|J=\frac{1}{2},\Omega=\frac{1}{2},M_J=\frac{1}{2}\rangle$ state a guiding field is installed. Inside the UHV chamber the orientation aperture is supplied with $U_{\text{orientation}}=\pm6.4$ kV. The positive or negative polarity of the field gives rise to N-end or O-end collisions, respectively. The Ni crystal is grounded to obtain a well defined homogeneous electric field of $F_{\text{orientation}}=8$ kV/cm at a distance of 8 mm between the aperture and the crystal. Two quadrupole mass analyzers (QMA) are mounted behind the target and therefore shielded from the direct beam. They are operated with the masses 28 and 30 for CO and NO, respectively. The chamber walls are saturated with NO, then the Ni(100) crystal is prepared, and afterwards the molecular beam is admitted to the UHV chamber. Neither NO nor CO can now be adsorbed on the chamber walls. Therefore, both QMA's detect only molecules leaving the surface. Using the four grid LEED optics, work function measurements $\Delta\Phi$ are carried out by means of a modified self-compensating retarding field (SCRF) method[39] combined with LEED and Auger electron spectroscopy (AES) in order to assess the part of molecularly adsorbed NO molecules on CO/Ni(100).[40] The sticking probability[41] of NO and the induced desorption of CO are determined from simultaneous measurements of the respective partial pressure using the two QMA's. The preparation of the Ni(100) crystal was carried out by Ar ion bombardment and heat treatment. After the cleaning process the properties of the surface were controlled by LEED and AES.

In order to ascertain its proper functioning, the state selection and focussing properties of the molecular beam part of the apparatus were investigated first. A characteristic focusing spectrum obtained by variation of the hexapole voltage is shown in Fig. 2. For this study, the crystal is substituted by an aperture and the direct beam was detected by one of the QMA's. In order to suppress background gas molecules the beam is modulated and analyzed by a lock in amplifier (LIA). Three different diameters of the aperture (1, 2, and 3 mm) were chosen while recording the intensity as a function of hexapole voltage U_{hex}. The LIA signal is normalized to the corresponding signals at $U_{\text{hex}}=0$ kV. Up to $U_{\text{hex}}=4$ kV the relative intensity stays almost constant due to the divergence of the NO beam leaving the nozzle. On increasing the voltage further, the ground state is focussed onto the target, and the intensity reaches its maximum at $U_{\text{hex}}=9.5$ kV, independent of the aperture. According to the LIA technique, the intensity relative to the background I_0 is found to be higher for a smaller aperture. Without the LIA the opposite occurs, since the QMA cannot distinguish between scattered and directly incoming molecules. The subsequent course indicates a second peak representing the next rotational state $|\frac{3}{2},\frac{1}{2},\frac{3}{2}\rangle$ with lower effective dipole moment at about $U_{\text{hex}}=16$ kV. All further experiments described in this paper were carried out at a fixed voltage of $U_{\text{hex}}=9.5$ kV focusing predominantly the ground state.

Figure 3 shows the two configurations of the NO molecular axis orientations which can be obtained for the two possible polarities of the electrical field $\vec{E}$ for the ideal case when all molecules are in the rotational ground state. For instance, the negative voltage (left) provides an "apple-shape" distribution with a high probability of O-end collisions and a vanishing small collision probability with the N-end towards the surface, and vice versa. This leads to a mean degree of orientation $\langle\cos\Phi\rangle = \frac{1}{3}$ for the ideal case, i.e., when only the ground state takes part. To obtain the

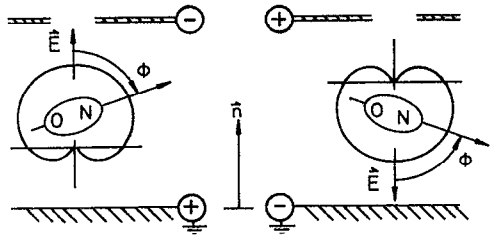

FIG. 3. Orientation distribution of the incoming NO molecules approaching the surface. Left side: Negative voltage at the orientation aperture ⇒ preferential O-end collisions: Right side: Positive voltage ⇒ preferential N-end collisions.

correct degree of orientation, one can vary the voltage of the orientation field and fit the theoretical course to the measured asymmetry, which has been done in our case,[15] resulting in an average orientation of $\langle\cos\Phi\rangle = 0.126 \pm 0.011$.

III. RESULTS

A. Work function measurements with unoriented NO molecules

To study the adsorption with regard to its dissociation behavior, the change of the work function during the coadsorption was measured while exposing the surface to unoriented molecules. The work function of the clean Ni(100) surface is given by $\Phi = 5.22 \pm 0.04$ eV.[42] In the left portion of Fig. 4, the change of the work function during CO exposure is shown. The increase of the work function after the CO coverage depends on the exposure. The final value obtained for the CO $c(2\times2)$ superstructure is $\Delta\Phi = 0.7$ eV which is in good agreement with the previous results.[29,42,43] This increase of $\Delta\Phi$ can be explained by the permanent dipole moment of the adsorbed diatomic molecules.[10] Comparing the data for the two temperatures, it is obvious that NO is less effective in displacing CO, since a higher exposure is needed to reach the final value. The data for the clean, partially covered and saturated surfaces reveals the dissociative character of NO on an unsaturated layer of CO caused by the increase of the number of dipoles. The subsequent decrease of the results is determined by the different amount of dissociation. The CO precoverage and temperature dependences of the resulting final values of the work function changes are shown in Table I. The value of the final work function depends on the initial CO exposure. The clean surface at $T = 300$ K yields a negative change of $\Delta\Phi = -0.1$ eV, whereas the fully CO $c(2\times2)$ precovered surface results in $\Delta\Phi = 0.25$ eV. At $T = 170$ K the resulting change of the work function is given by approximately $\Delta\Phi = 0.3$ eV, independent of the CO precoverage. The results for the clean Ni(100) and their interpretation have already been reported.[32] $\Delta\Phi$ is indicative of the degree of molecular adsorption.[40] It would appear that the CO precoverage on the Ni(100) surface reduces the dissociation of the adsorbing molecules. Unfortunately, the total amount of dissociated molecules cannot be determined by the $\Delta\Phi$ measurements. Saturation coverage of CO implies a work function change of $\Delta\Phi = 0.25$ eV for the NO on the CO $c(2\times2)$/Ni(100) system at 300 K, which is

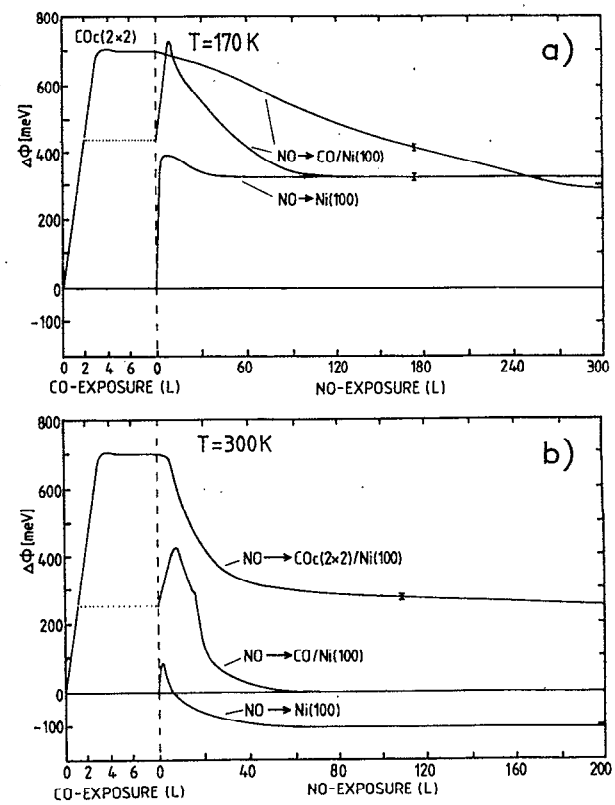

FIG. 4. Changes of work function of NO on clean, partially precovered and fully CO precovered Ni(100) measured at (a) $T = 170$ K and at (b) 300 K.

almost as high as for the same system at 170 K. This indicates therefore that the adsorption of NO on a CO $c(2\times2)$/Ni(100) surface proceeds mainly molecularly even at a substrate temperature at 300 K. The initial dipole moment and the polarizabilities of the molecules can be determined from the $\Delta\Phi$ measurements during the adsorption at the clean surface. Therefore, we fitted the data for low coverages to a Topping model.[44] The initial dipole moment of NO was found to be $p_0 = 0.25 \pm 0.01$ D, and the effective polarizability $\alpha_e = 2.6 \pm 0.3$ Å^3 independent of the temperature, assuming a constant initial sticking probability near unity. For CO values of $p_0 = 0.34 \pm 0.02$ D and $\alpha_e = 3.25 \pm 0.2$ Å^3 at an initial sticking probability of 0.9 (Ref. 45) were found. These results are in good agreement with the literature for both molecules.[45,46] The signs of the dipole moments are reversed compared to the molecule in the gas phase and the polariz-

TABLE I. Final change of work function for NO on CO/Ni(100) as a function of temperature and precoverage.

	Final work function change (meV) CO precoverage (Θ_{CO}/Θ_{max})			
Temperature (K)	0	1/3	2/3	1
115	745			
170	320		320	290
300	−110	0		250

ability is greater. The different sign of the dipole moment of adsorbed molecules is due a change in the electron density of the molecular orbitals as discussed by various authors.[47–49] The LEED patterns observed showed no evidence for dissociation. AES indicates that the carbon is not completely removed at temperatures below 200 K and an increasing amount of carbon is obtained at lower temperatures. Therefore, we conclude that at 300 K the displacement of CO is complete and the sticking of NO is mainly molecular. A similar displacement was observed by Conrad *et al.*[50] From the change in their ultraviolet photoelectron spectra (UPS), the authors infer that NO is displaced from Pd by CO molecules. Deviations between molecular beam experiments (as described in Sec. III B) and diffuse exposure experiments occur due to the lower kinetic and rotational energy of the NO molecules.

B. NO sticking and CO desorption by unoriented NO molecules

As outlined previously,[15,16] in order to obtain the sticking probability we used the reflector technique first described by King and Wells.[41] At $T=300$ K the fully CO precovered surface is exposed to the NO beam and the partial pressure within the vacuum chamber is recorded. The NO signal given in Fig. 5(a) therefore arises from the NO molecules which do not stick. After 15 min the NO pressure reaches a constant value since the surface is then saturated with NO. The NO signal is given by the amount of scattered and desorbed molecules, the latter arising from the trapping/desorption channel. The marked area above the curve represents the amount of the adsorbed NO molecules. The sticking probability S can be calculated by dividing the difference between the partial pressure, $p_{NO}(t)$ and the saturation value p_e by the marked area, resulting in

$$S(t)=1-\frac{p_{NO}(t)}{p_e}. \tag{1}$$

As a function of time, the change of the NO coverage normalized to the saturation coverage is given by

$$\frac{\Theta_{NO}(t)}{\Theta_{NO}^{sat}}=S(t)\Big/\int_0^\infty S(t)dt. \tag{2}$$

The saturation coverage for NO at Ni(100) is 8.9×10^{18} molecules/m^2, corresponding to a $c(2\times2)$ adlayer.

Simultaneously, the signal of the desorbed CO molecules is recorded with a second QMA. After 20 s the CO signal reaches its maximum and after 2 min it is no longer detectable, indicating that nearly all CO molecules are desorbed. Reaction products such as N_2 or CO_2 could not be detected. The CO signal in Fig. 5(a) is normalized to the area for the sticking NO molecules, since the saturated adsorption layers for both CO and NO contain almost the same amount of molecules, each exhibiting a $c(2\times2)$ superstructure.[32,43] In addition, AES does not show any detectable carbon signal indicating that carbon is completely removed from the surface. This allows definition of the coefficient D_s describing

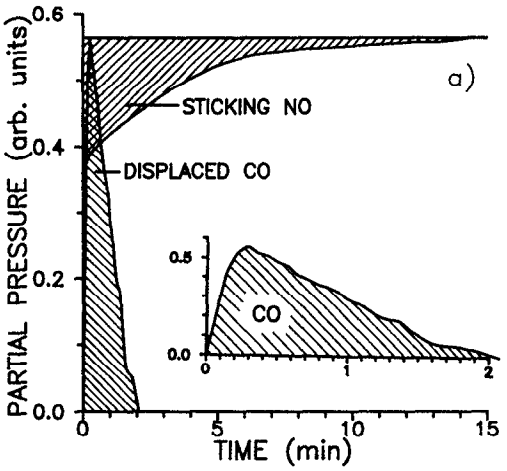

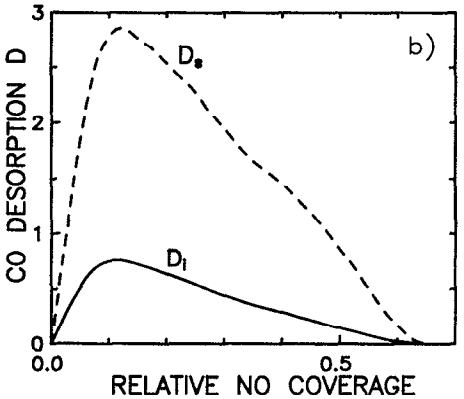

FIG. 5. (a) NO and CO partial pressures measured as a function of time during the desorption process. The dashed areas represent saturation coverages of NO and CO on Ni(100). (b) Number of CO molecules desorbed by each sticking NO molecule (dashed curve) and by each incoming NO molecule (solid curve=dashed curve multiplied by the sticking probability) as a function of NO coverage.

the amount of desorbed CO molecules with respect to the sticking NO molecules in close analogy to the sticking probability as being

$$\begin{aligned} D_s(t)&=-\frac{d\Theta_{CO}(t)}{d\Theta_{NO}(t)}\\ &=-\frac{\dot{\Theta}_{CO}(t)}{\dot{\Theta}_{NO}(t)}\\ &=\frac{p_{CO}(t)}{S(t)}\left(\int_0^\infty S(t)dt\Big/\int_0^\infty p_{CO}dt\right). \end{aligned} \tag{3}$$

On the other hand, the time dependence of the CO coverage can be determined from the CO partial pressure p_{CO} and the absolute NO exposure I_0. From this the desorption probability D_i, describing the amount of desorbed CO molecules with respect to each incoming molecule can be derived

$$D_i(t)=-\frac{\Theta_{CO}(t)}{I_0}=p_{CO}\left(\int_0^\infty S(t)dt\Big/\int_0^\infty p_{CO}dt\right). \tag{4}$$

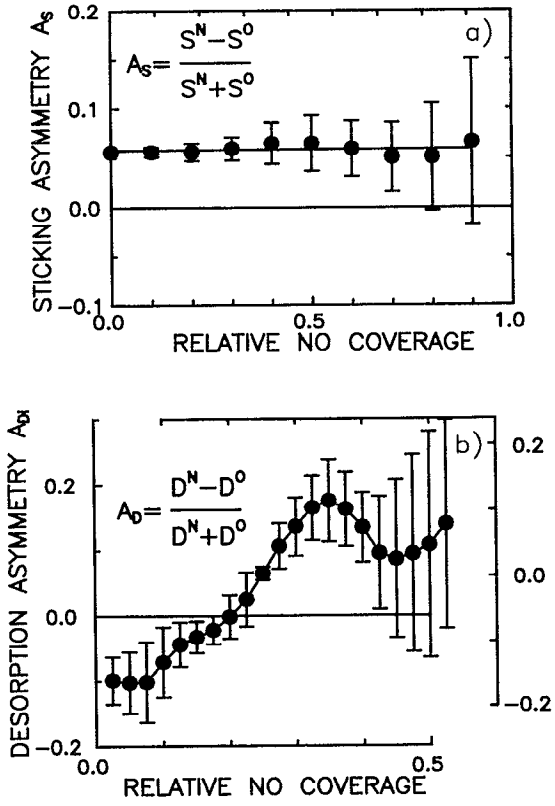

FIG. 6. Orientation asymmetry of the (a) NO sticking and (b) CO desorption at CO/Ni(100) as a function of NO coverage. In (b) the left asymmetry scale refers to each incoming; the right scale to each sticking NO molecule.

By a time integration of $S(t)$ and $D(t)$ the relative coverages of NO and CO can be obtained as a function of time. Consequently, $S(t)$ and $D(t)$ as well as the corresponding asymmetries can be converted into the dependences of Θ_{NO} as shown in Fig. 5(b) and Fig. 6. "Relative" NO coverage in these figures means that the given values are normalized to the $c(2\times2)$ saturation coverage of NO occupying 50% of the nickel sites. The CO desorption coefficient D_s and the CO desorption probability D_i are given in Fig. 5(b) as a function of the NO coverage for unoriented molecules. The CO desorption was found to increase up to a maximum at $\Theta_{NO}=0.1$, corresponding to $\Theta_{CO}=0.8$. Here, on average, almost 3 CO molecules desorb, activated by each adsorbed NO molecule, or 0.8 CO molecules desorb, activated by each incoming NO molecule. At NO coverages higher than 0.6, the CO signal is no longer detectable, indicating that the CO coverage becomes negligibly small. Such a kind of desorption/displacement was investigated by Hamza *et al.*[24] for the same system at a substrate temperature of $T=140$ K. For the desorption/displacement coefficient D_s they found, at $\Theta_{NO}=0$ and $\Theta_{CO}=1$, a steep increase followed by an exponential decrease of the CO desorption as function of time.[51] In contrast to the data observed here, a distinct rise time was not detectable within the time resolution of their experiments, which can lead to the assumption that a one-by-one exchange of CO and NO occurred and the process can be described as displacement. In contrast to this displacement, the slow rise of the data shown in Fig. 5(a) at $T=300$ K indicates that an additional process is in effect here (see the following).

C. NO sticking and CO desorption by oriented NO molecules

The sticking and the desorption data were recorded for both possible orientations, namely preferential N-end and O-end collisions with the CO $c(2\times2)$/Ni(100) surface. To discuss the orientation dependent results we define an asymmetry A_I:

$$A_I = \frac{I^N - I^O}{I^N + I^O}, \tag{5}$$

where I is one of the measurands S, D_s, or D_i. A positive value of the asymmetry A_I means that the sticking or desorption probability is higher for preferential N-end collisions corresponding to the favored adsorption configuration of the NO adsorbates. If twice the value obtained for unoriented molecules $2\times I^U$ is equal to the sum of the intensities measured for oriented molecules $I^N + I^O$, then this asymmetry is equal to the steric effect as defined by the Kleyn group.[5,6] In this case we can normalize the asymmetry to the mean degree of orientation. However, if an alignment plays an important role, then this relation may not generally be valid.[38]

In Fig. 6(a) the sticking asymmetry $A_S(\Theta)$ is shown as a function of the NO coverage. The asymmetry is given by its initial value, almost independent of the coverage. This behavior can be explained by the influence of the direct NO chemisorption. Therefore, we deduce a large amount of directly chemisorbed NO molecules in spite of the fact that the surface is precovered with a monolayer of CO. Figure 6(b) shows the asymmetry of the CO desorption referring to each incoming NO molecule as a function of the relative NO coverage. The asymmetry rises from -0.1 at low coverage to a maximum of 0.17 at $\Theta_{NO}=0.35$. The scale on the right hand side represents the asymmetry of the CO desorption referring to each stuck NO molecule. The two scales A_{Di} and A_{Ds} can be converted into each other:

$$A_s = \frac{S^N - S^O}{S^N + S^O}. \tag{6}$$

This leads to

$$S^N = \tfrac{1}{2} S^U (1 + A_s), \tag{7}$$

$$S^O = \tfrac{1}{2} S^U (1 - A_s), \tag{8}$$

using S^U, which is the sticking probability for unoriented (random) collisions and therefore, the arithmetic mean of S^N and S^O. The desorption asymmetry A_{Ds} corresponding to the NO molecules stuck on the surface and the resulting A_{Di} corresponding to each incoming NO molecule can be written as

$$A_{Ds} = \frac{D^N - D^O}{D^N + D^O}, \tag{9}$$

$$A_{Di} = \frac{D^N S^N - D^O S^O}{D^N S^N + D^O S^O}, \tag{10}$$

TABLE II. Parameters describing the coverage dependency of the sticking probability fitted to an extended Kisliuk model.

		Adsorption parameters N-end	O-end
$T=155$ K	S_0	0.467±0.002	0.379±0.002
Ni(100) clean	k	0.37 ±0.03	0.37 ±0.03
	h	0.012±0.005	0.019±0.005
$T=300$ K	S_0	0.31 ±0.001	0.277±0.001
Ni(100)+CO	k	0.31 ±0.003	0.31 ±0.003
	h	−0.125±0.002	−0.126±0.002

A_{Di} can be transformed using Eqs. (7) and (8) into

$$A_{Di}=\frac{A_{Ds}+A_s}{1+A_sA_{Ds}}. \tag{11}$$

Since A_sA_{Ds} is negligibly small, the relation can be simplified as

$$A_{Di}\cong A_{Ds}+A_s. \tag{12}$$

Therefore the right scale (stuck NO molecules) in Fig. 6(b) is shifted by the constant coverage independent value of the NO sticking asymmetry of 0.06, as given in Fig. 6(a).

IV. DISCUSSION

We fitted the values obtained for the dependence of the sticking probability as a function of the NO coverage Θ to an extended Kisliuk model, taking into account direct chemisorption and also different values for the probabilities of trapping to the intrinsic or the extrinsic precursor state, as described previously:[15,38]

$$S(\Theta)=\frac{S_0+h\Theta}{1+k\Theta/(1-\Theta)}. \tag{13}$$

The initial sticking probability S_0 includes direct chemisorption as well as indirect adsorption via an intrinsic precursor state. The constant k remains the same as in the original work of Kisliuk.[51,52] It describes the exchange of molecules between the precursor states by diffusion of the adsorbed molecules and therefore cannot depend on the orientation of the molecules prior to the collision. The additional constant h depends on the direct chemisorption as well as on the trapping to the precursor states, therefore, it may be orientation dependent. The results obtained from the fit are given in Table II and are compared to the values for a clean surface determined from the data of Ref. 15.

As discussed earlier, in the context of the $\Delta\Phi$ measurements, both experiments at low temperatures (clean surface) and at room temperature (CO precovered surface) lead to an almost equivalent state of the surface. This means that one has nearly the same amount of dissociated molecules on the saturated NO/Ni(100) surface in both cases. The k values in Table II are not very different. This indicates that the diffusion between the intrinsic and the extrinsic precursor state is not influenced drastically by the CO precoverage. The differences can be attributed to the change in temperature in the two experiments, because the rate coefficients for the diffusion between the precursor states are temperature dependent. The initial sticking probability S_0 as well as the constant h have lower values for the coadsorption case, indicating that the probability for direct chemisorption, the trapping probabilities, or both, are influenced by the preadsorbed CO molecules. The decrease of the initial sticking probability is stronger than expected from a pure temperature effect. For unoriented molecules we measured a value of $S_0=0.37$ at $T=300$ K without CO preadsorption. This can be explained by the fact that the number of free adsorption sites for direct NO chemisorption is reduced significantly at the CO covered Ni(100) surface. As obtained from the orientation-dependent values, the initial sticking asymmetry decreases from $A_s=0.09\pm0.01$ (Refs. 15 and 16) for the clean surface to $A_s=0.056\pm0.005$ for the CO precovered one. This demonstrates the decrease of direct chemisorption. The interdependence of h, direct chemisorption, and trapping is too complicated to be analyzed without detailed knowledge of the interaction process. Unfortunately, NO scattering experiments cannot be performed at the CO $c(2\times2)$/Ni(100) surface, due to the high CO desorption probability.

For further discussion of the coadsorption dynamics, in particular, with respect to the orientation asymmetry, we interpret the results displayed in Figs. 5 and 6 as follows. Since the sticking and the CO displacement do not have the same trend and sign at all NO coverages, the displacement process cannot only depend on the sticking. Rather, two different kinds of processes superpose. The first process is based on the change of the electronic state within the Ni surface during the NO adsorption. The adsorbed NO molecules cause a charge shift towards the N atoms.[53] At higher coverages more NO molecules are next to a CO molecule, resulting in a lower d-electron density underneath the CO. Since this electron density is responsible for the bonding,[29,30] the bond is weakened and CO can desorb via a precursor state. This process depends on the amount of chemisorbed NO *and* CO molecules and can be described by a differential equation of the form $\dot{\Theta}_{CO}\sim\Theta_{CO}\cdot\Theta_{NO}$.[54] This equation is coupled to the sticking probability [see Eq. (13)] and the Θ_{CO} dependent reduction of S_0. The solution describes the experimental data and the desorption asymmetry qualitatively. The CO molecules undergo a transition from the chemisorbed state to the weakly bound intrinsic precursor from which they may be desorbed thermally. However, the results for our measurements suggest that there is an additional mechanism effective here. This second process, proposed by Hamza *et al.*,[24] involves the displacement of CO by NO from the extrinsic precursor. These authors investigated at the same adsorption system 140 °C and explained it by a one-by-one exchange of CO and NO molecules:

$$NO_g+CO_c=NO_{ex}+CO_c=NO_c+CO_{ex}=NO_c+CO_g, \tag{14}$$

where the subscripts g, c, and ex stand for the gas phase, chemisorbed, and extrinsic precursor states, respectively. This mechanism prevails at low NO coverages and may be expected to be orientation independent. Nevertheless, we observed a slightly negative course up to an NO coverage of 0.2 [see Fig. 6(b)]. It may be that the asymmetric shape of the NO electronic charge distribution is responsible for a higher trapping probability in favor of O-end collisions,[4,53]

Transfer of translational energy into rotational energy can occur very efficiently from NO molecules to CO molecules in the intrinsic precursor state. This would describe a direct displacement of CO by the NO molecules not chemisorbed. The NO molecules pointing with the O-end to the surface gain rotational energy and kick out the chemisorbed CO molecules. This is more effective for O-end collisions, since the molecules reach the surface with the wrong sticking configuration. At the clean Ni(100) surface these molecules cannot transfer the rotational energy to the substrate. They are trapped but cannot be adsorbed. These rotating molecules need more space during the adsorption process at the precovered surface compared with the molecules hitting the surface with the N-end, resulting in a higher effective cross section for NO–CO collisions. This could cause the measured negative displacement asymmetry at the beginning of the process as well as the reduced sticking asymmetry compared to the value obtained without precoverage.

V. CONCLUSION

In conclusion, first investigations of the collision between two oriented molecules were carried out. We found strong orientation asymmetries both in the sticking and desorption process reflecting the directional properties of the adsorption potentials involved. From the orientation-dependent measurements we conclude that two different mechanisms participate in the desorption process. We conclude that a direct and an indirect mechanism are responsible for the change of sign of the displacement/desorption asymmetry. For O-end collisions a direct displacement prevails, whereas for N-end collisions the higher sticking probability leads to a NO-induced CO desorption from the chemisorbed state.

ACKNOWLEDGMENT

The authors thank M. Volkmer for assistance during the $\Delta\Phi$ measurements. Financial support by DFG(SFB 216) and the Commission of the European Communities is gratefully acknowledged.

[1] K. H. Kramer and R. B. Bernstein, J. Chem. Phys. **42**, 767 (1965).
[2] D. H. Parker and R. B. Bernstein, Annu. Rev. Phys. Chem. **40**, 561 (1989).
[3] M. G. Tenner, E. W. Kuipers, W. Y. Langhout, A. W. Kleyn, B. Nicolasen and S. Stolte, Surf. Sci. **236**, 151 (1990).
[4] M. G. Tenner, E. W. Kuipers, A. W. Kleyn, and S. Stolte, J. Chem. Phys. **89**(10), 6552 (1988).
[5] E. W. Kuipers, M. G. Tenner, A. W. Kleyn, and S. Stolte, Phys. Rev. Lett. **62**, 2152 (1989).
[6] E. W. Kuipers, M. G. Tenner, A. W. Kleyn, and S. Stolte, Nature **334**, 420 (1988).
[7] M. Tenner, F. H. Geuzebroek, E. W. Kuipers, A. E. Wiskerke, W. Kleyn, and S. Stolte, Chem. Phys. Lett. **168**, 45 (1990).
[8] E. W. Kuipers, M. G. Tenner, A. W. Kleyn, and S. Stolte, Surf. Sci. **211/212**, 819 (1989).
[9] E. W. Kuipers, M. G. Tenner, A. W. Kleyn, and S. Stolte, Chem. Phys. **138**, 451 (1989).
[10] E. W. Kuipers, M. G. Tenner, A. W. Kleyn, and S. Stolte, J. Vac. Sci. Technol. A **8**(3), 2692 (1990).
[11] A. W. Kleyn, E. W. Kuipers, M. G. Tenner, and S. Stolte, J. Chem. Soc. Faraday Trans. 2 **85**(8), 1337 (1989).
[12] R. S. Mackay, T. J. Curtiss, and R. B. Bernstein, J. Chem. Phys. **92**, 801 (1989).
[13] T. J. Curtiss and R. B. Bernstein, Chem. Phys. Lett. **161**, 212 (1989).
[14] R. S. Scott, T. J. Curtiss, and R. B. Bernstein, Chem. Phys. Lett. **164**, 341 (1989).
[15] G. H. Fecher, N. Böwering, M. Volkmer, B. Pawlitzky, and U. Heinzmann, Surf. Sci. Lett. **230**, L169 (1990).
[16] G. H. Fecher, M. Volkmer, B. Pawlitzky, N. Böwering, and U. Heinzmann, Vacuum **41**, 265 (1990).
[17] G. H. Fecher, M. Volkmer, N. Böwering, B. Pawlitzky, and U. Heinzmann, J. Chem. Soc. Faraday Trans. 2 **85**(8), 1364 (1989).
[18] H. Müller, B. Dierks, F. Hamza, G. Zagatta, G. H. Fecher, N. Böwering, and U. Heinzmann, Surf. Sci. **269/270**, 207 (1992).
[19] D. Lemoine and G. C. Corey, J. Chem. Phys. **94**, 767 (1991).
[20] S. Holloway and D. Halstedt, Chem. Phys. Lett. **154**, 181 (1989).
[21] G. C. Corey and D. Lemoine, Chem. Phys. Lett. **160**, 324 (1989).
[22] S. B. Schwartz and L. D. Schmidt, Surf. Sci. **206**, 169 (1988).
[23] S. B. Schwartz, G. B. Fisher, and L. D. Schmidt, J. Phys. Chem. **92**, 389 (1988).
[24] A. V. Hamza, P. M. Ferm, F. Budde, and G. Ertl, Surf. Sci. **199**, 13 (1988).
[25] S. Andersson and J. B. Pendry, J. Phys. C **13**, 3547 (1980).
[26] H. C. Poon and D. K. Saldin, J. Phys. Condens. Matt. **1**, 1551 (1989).
[27] S. Y. Tong, A. Maldonado, C. H. Li, and M. A. Hove, Surf. Sci. **94**, 73 (1980).
[28] C. L. Allyn, T. Gustafsson, and E. W. Plummer, Chem. Phys. Lett. **47**, 127 (1977).
[29] E. Wimmer, C. L. Fu, and A. J. Freeman, Phys. Rev. Lett. **55**, 2618 (1985).
[30] G. Blyholder, J. Vac. Sci. Technol. **11**, 865 (1974).
[31] Shikong Shen, P. Feulner, E. Umbach, W. Wurth, and D. Menzel, Z. Naturforsch. **42a**, 1333 (1987).
[32] M. Volkmer, K. Nolting, G. H. Fecher, B. Dierks, and U. Heinzmann, Vacuum **41**, 109 (1990).
[33] J. Stöhr and R. Jaeger, Phys. Rev. B **26**, 4111 (1982).
[34] A. Sandell, A. Nilsson, and N. Mårtensson, Surf. Sci. Lett. **241**, L1 (1991).
[35] A. Sandell, A. Nilsson, and N. Mårtensson, Surf. Sci. **251/252**, 971 (1991).
[36] G. Odörfer, R. Jaeger, G. Illing, H. Kuhlenbeck, and H.-J. Freund, Surf. Sci. **233**, 44 (1990).
[37] C. Westphal, PhD. thesis, Universität Bielefeld, 1992.
[38] G. H. Fecher, PhD. thesis, Universität Bielefeld, 1990.
[39] R. Nathan and B. J. Hopkins, J. Phys. E **7**, 851 (1974).
[40] J. C. Tracy, J. Chem. Phys. **56**, 2748 (1972).
[41] D. A. King and M. G. Wells, Surf. Sci. **29**, 454 (1972).
[42] J. Hölzl and F. K. Schulte, *Solid Surface Physics* (Springer, Berlin, 1979).
[43] S. Andersson and J. B. Pendry, Surf. Sci. **71**, 75 (1978).
[44] M. Volkmer, thesis, Universität Bielefeld, 1990.
[45] J. C. Campuzano, R. Dus, and R. G. Greenler, Surf. Sci. **102**, 172 (1981).
[46] K. Akimoto, Y. Sakisaka, M. Nishijima, and M. Onchi, Surf. Sci. **88**, 109 (1979).
[47] H. Ibach and H. Lüth, *Festkörperphysik* (Springer, Berlin, 1988).
[48] F. Zaera and D. D. Fischer, Surf. Sci. **194**, 205 (1988).
[49] B. E. Koel, D. E. Peebles, and J. M. White, Surf. Sci **125**, 709 (1983).
[50] H. Conrad, G. Ertl, J. Küppers, and E. E. Latta, Faraday Disc. Chem. Soc. **58**, 116 (1974).
[51] P. Kisliuk, J. Phys. Chem. Solids **3**, 95 (1957).
[52] P. Kisliuk, J. Phys. Chem. Solids **5**, 78 (1958).
[53] A. Schichl and N. Rösch, Surf. Sci. **137**, 261 (1984).
[54] U. P. Zhdanov, *Elementary Physicochemical Processes on Solid Surfaces* (Plenum, New York, 1991).